CONSTANT MODULUS PROBING WAVEFORM DESIGN FOR MIMO RADAR VIA ADMM ALGORITHM

Yongchao Wang, Jiangtao Wang

State Key Laboratory of Intergrated Services Networks
Xidian University, Xi'an, China

ABSTRACT

In this paper, we design constant modulus probing waveforms with low correlation sidelobes for colocated multi-input multi-output (MIMO) radar. Through exploiting the structure of the problem, we formulate it as a non-convex consensus minimization problem. Then a customized alternating direction method of multipliers (ADMM) algorithm is proposed to solve the problem, which is guaranteed convergent to its stationary point. Numerical examples show that the proposed approach offers better performance than the state-of-the-art approaches. Moreover, parallel implementation structure indicates that the proposed ADMM algorithm is suitable for applications involving large dimensionality.

Index Terms— Constant modulus probing waveform, beam pattern, MIMO radar, auto-/cross-correlation, ADMM.

1. INTRODUCTION

Compared to phased-array radar, colocated multi-input multi-output (MIMO) radar system enjoys the advantage of waveform diversity [1], [2], which can generate desired transmission beampatterns, improving the directional resolution of the system and suppressing the interference [3], [4]. In colocated MIMO radar system, a key research topic is to design constant modulus probing waveforms efficiently according to practical applications, which has attracted a lot of attentions in recent years [5]-[10]. In [8], a cyclic algorithm (CA) is proposed to synthesize constant modulus waveform and pursue both auto- and cross-correlation properties. A coordinate-descent framework to design low PSL/ISL sequences is dealt with in [9], which only considers autocorrelation properties. In [10], the authors propose a double alternating direction method of multipliers (D-ADMM) algorithm to minimize the absolute-error between the designed beampattern and the given beampattern.

In this paper, we still focus on this issue and design desired beampatterns using constant modulus waveforms with low spacial auto- and cross-correlation sidelobes. Through exploiting the problem's structure, it is modeled as a non-convex consensus minimization problem. Different from the previous works in [5]-[10], it is the first time that this design problem is formulated into a separable problem including many parallel subproblems. To efficiently solve these non-convex subproblems, we propose a customized consensus-ADMM algorithm. In it, all subproblems except one subproblem can be performed independently, which results in much flexibility and efficiency from a practical point of view. Moreover, the proposed consensus-ADMM algorithm is guaranteed convergent to some stationary point of the original non-convex problem. Furthermore, Nesterov's accelerated gradient descent (AGD) method [11] and statistics gradient descent (SGD) method [12] are adopted to improve the performance of our proposed consensus-ADMM algorithm. Numerical simulation results show that the proposed approaches compare favorably with the state-of-the-art approaches in terms of both algorithm computational complexity and the spacial correlation sidelobes.

This work was supported in part by the National Natural Science Foundation of China under Grant 61771356 and 111 project of China under grant B08038.

2. PROBLEM FORMULATION

Consider a colocated MIMO radar system equipped with M antennas in a uniform linear array. In the system, we set the inter-element spacing $d = \frac{\lambda}{2}$, where λ is the signal wavelength. The spacial direction θ belongs to the angle set Θ. The steer vector $\mathbf{a} \in \mathbb{C}^M$ at direction θ is given by

$$\mathbf{a}_\theta = \left[1, e^{j2\pi d \sin(\theta)/\lambda}, \cdots, e^{j2\pi(M-1)d\sin(\theta)/\lambda}\right]^T. \quad (1)$$

The probing waveform transmitted by the m-th antenna is denoted by $\mathbf{x}_m = [x_m(1), \cdots, x_m(N)]^T, m = 1, \cdots, M$. Then, the waveforms transmitted by the MIMO radar system can be expressed as the following N-by-M matrix

$$\mathbf{X} = [\mathbf{x}_1, \cdots, \mathbf{x}_M]. \quad (2)$$

The synthesized signal at the spacial direction θ is $\mathbf{X}\mathbf{a}_\theta$. Then, the beampattern, which describes the power distribution at the spacial direction θ can be described by

$$P_\theta = \mathbf{a}_\theta^H \mathbf{X}^H \mathbf{X} \mathbf{a}_\theta. \quad (3)$$

Let $\mathbf{S}_n$ denote an off-line diagonal matrix, where n denotes the delay parameter. Then, the time-delayed waveform can be expressed by $\mathbf{S}_n\mathbf{X}\mathbf{a}_\theta$. The spacial correlation of the waveform and its delayed version can be defined as

$$P_{\theta_i,\theta_j,n} = \mathbf{a}_{\theta_i}^H \mathbf{X}^H \mathbf{S}_n \mathbf{X} \mathbf{a}_{\theta_j}, \quad (4)$$

where $\theta_i, \theta_j \in \hat{\Theta} \subset \Theta$ and $\hat{\Theta} = \{\theta_1, \cdots, \theta_K\}$ is the angle set of the desired beampatterns.

In this paper, we design desired beampatterns using constant modulus waveforms with low spacial auto- and cross-correlation sidelobes. To reach this goal, we develop the following optimization model

$$\begin{aligned} &\min_{\alpha, \mathbf{X}} \ \ \omega^2 e(\alpha, \mathbf{X}) + \omega_c^2 P_c(\mathbf{X}), \\ &\text{s.t.} \ \ |x_m(n)| = 1, n = 1, \cdots, N; m = 1, \cdots, M, \end{aligned} \tag{5}$$

where

$$e(\alpha, \mathbf{X}) = \sum_{\theta \in \Theta} |\alpha \bar{P}_\theta - \mathbf{a}_\theta^H \mathbf{X}^H \mathbf{X} \mathbf{a}_\theta|^2, \tag{6a}$$

$$P_c(\mathbf{X}) = \sum_{n \in \mathcal{T} \backslash 0} \sum_{\theta_i \in \hat{\Theta}} |P_{\theta_i, \theta_i, n}|^2 + \sum_{n \in \mathcal{T}} \sum_{\substack{\theta_i \neq \theta_j \\ \theta_i, \theta_j \in \hat{\Theta}}} |P_{\theta_i, \theta_j, n}|^2, \tag{6b}$$

ω and ω_c are preset positive real weights and $\mathcal{T}$ is the temporal delay parameter set of interest. In (5)'s objective function, the first term $e(\alpha, \mathbf{X})$ represents the mismatching square error between the designed beampattern and the desired beampattern $\bar{P}_\theta$. The second term $P_c(\mathbf{X})$ is the spacial correlation function, which describes the auto- and cross-correlation sidelobes at spacial directions of interest. α is a positive scaling variable to be optimized.

Since every element in $\mathbf{X}$ is constant modulus, we can drop the non-convex constant modulus constraints through letting $\mathbf{X}$'s phase $\mathbf{\Phi}$ be variable and rewrite (5) as an unconstrained minimization problem

$$\min_{\alpha, \mathbf{\Phi}} \ \ \omega^2 e(\alpha, \mathbf{X}(\mathbf{\Phi})) + \omega_c^2 P_c(\mathbf{X}(\mathbf{\Phi})). \tag{7}$$

Moreover, we define the following quantities

$$\begin{aligned} &\mathbf{a}_{\theta,\theta} = \text{vec}(\mathbf{a}_\theta \mathbf{a}_\theta^H), \quad p = \sum_{\theta \in \Theta} \bar{P}_\theta, \\ &\mathbf{q} = -\sum_{\theta \in \Theta} \bar{P}_\theta \mathbf{a}_{\theta,\theta}, \quad \mathbf{A} = \sum_{\theta \in \Theta} \mathbf{a}_{\theta,\theta} \mathbf{a}_{\theta,\theta}^H. \end{aligned} \tag{8}$$

Then, the first term in (7) can be equivalent to

$$\omega^2 e(\alpha, \mathbf{\Phi}) = \mathbf{v}^H(\alpha, \mathbf{\Phi}) \mathbf{Q} \mathbf{v}(\alpha, \mathbf{\Phi}), \tag{9}$$

where

$$\mathbf{v}(\alpha, \mathbf{\Phi}) = \begin{bmatrix} \alpha \\ \text{vec}\left(\mathbf{X}^H(\mathbf{\Phi}) \mathbf{X}(\mathbf{\Phi})\right) \end{bmatrix}, \mathbf{Q} = \omega^2 \begin{bmatrix} p & \mathbf{q}^H \\ \mathbf{q} & \mathbf{A} \end{bmatrix}.$$

In addition, define matrices $\mathbf{B}_n(\mathbf{\Phi})$, for $n = 0$

$$\mathbf{B}_n(\mathbf{\Phi}) = \begin{bmatrix} 0, & P_{\theta_1, \theta_2, n} & \cdots & P_{\theta_1, |\hat{\Theta}|, n} \\ \vdots & \ddots & \vdots & \vdots \\ P_{|\hat{\Theta}|, \theta_1, n} & P_{|\hat{\Theta}|, \theta_2, n} & \cdots & 0 \end{bmatrix},$$

and for $n \in \mathcal{T} \backslash 0$

$$\mathbf{B}_n(\mathbf{\Phi}) = \begin{bmatrix} P_{\theta_1, \theta_1, n} & P_{\theta_1, \theta_2, n} & \cdots & P_{\theta_1, |\hat{\Theta}|, n} \\ \vdots & \ddots & \vdots & \vdots \\ P_{|\hat{\Theta}|, \theta_1, n} & P_{|\hat{\Theta}|, \theta_2, n} & \cdots & P_{|\hat{\Theta}|, |\hat{\Theta}|, n} \end{bmatrix}.$$

where $|\hat{\Theta}|$ is the set $\hat{\Theta}$'s size. Then, $P_c(\mathbf{X}(\mathbf{\Phi}))$ in (7) can be rewritten as

$$P_c(\mathbf{X}(\mathbf{\Phi})) = \sum_{n \in \mathcal{T}} \|\mathbf{B}_n(\mathbf{\Phi})\|_F^2. \tag{10}$$

Combing (9) and (10), we can obtain the following compact form of objective function

$$\omega^2 e(\alpha, \mathbf{X}(\mathbf{\Phi})) + \omega_c^2 P_c(\mathbf{X}(\mathbf{\Phi})) = h(\alpha, \mathbf{\Phi}) + \sum_{n \in \mathcal{T}} f_n(\mathbf{\Phi})$$

where

$$h(\alpha, \mathbf{\Phi}) = \mathbf{v}^H(\alpha, \mathbf{\Phi}) \mathbf{Q} \mathbf{v}(\alpha, \mathbf{\Phi}), \tag{11a}$$

$$f_n(\mathbf{\Phi}) = \omega_c^2 \|\mathbf{B}_n(\mathbf{\Phi})\|_F^2. \tag{11b}$$

Then, the problem (7) can be equivalent to the following consensus problem by introducing a set of auxiliary variables $\{\mathbf{\Phi}_n | n \in \mathcal{T}\}$

$$\begin{aligned} &\min_{\alpha, \{\mathbf{\Phi}, \mathbf{\Phi}_n\} \in \mathbb{R}^{N \times M}} h(\alpha, \mathbf{\Phi}) + \sum_{n \in \mathcal{T}} f_n(\mathbf{\Phi}_n), \\ &\text{s. t.} \qquad \mathbf{\Phi}_n = \mathbf{\Phi}, \ \ n \in \mathcal{T}. \end{aligned} \tag{12}$$

In comparison with (7), the model (12) allows each subfunction $f_n(\mathbf{\Phi}_n)$ to handle its local variable $\mathbf{\Phi}_n$ independently. Through exploiting this kind of structure, we develop an efficient parallel and theoretically convergence guaranteed solving algorithm for the optimization problem. To the best of my knowledge, it is the first time that parallel algorithm structure is introduced to match the desired spacial beampattern in the MIMO radar system.

3. CUSTOMIZED CONSENSUS-ADMM SOLVING ALGORITHMS

The augmented Lagrangian function of the problem (12) can be written as

$$\begin{aligned} &\mathcal{L}(\alpha, \mathbf{\Phi}, \{\mathbf{\Phi}_n, \mathbf{\Lambda}_n | n \in \mathcal{T}\}) = h(\alpha, \mathbf{\Phi}) \\ &+ \sum_{n \in \mathcal{T}} \left[f_n(\mathbf{\Phi}_n) + \langle \mathbf{\Lambda}_n, \mathbf{\Phi}_n - \mathbf{\Phi} \rangle + \frac{\rho_n}{2} \|\mathbf{\Phi}_n - \mathbf{\Phi}\|_F^2 \right], \end{aligned} \tag{13}$$

where $\{\mathbf{\Lambda}_n | n \in \mathcal{T}\}$ are Lagrangian multipliers and $\{\rho_n | n \in \mathcal{T}\}$ are corresponding penalty parameters. We define

$$\mathcal{L}_n(\mathbf{\Phi}, \mathbf{\Phi}_n, \mathbf{\Lambda}_n) = f_n(\mathbf{\Phi}_n) + \langle \mathbf{\Lambda}_n, \mathbf{\Phi}_n - \mathbf{\Phi} \rangle + \frac{\rho_n}{2} \|\mathbf{\Phi}_n - \mathbf{\Phi}\|_F^2.$$

Then, the consensus-ADMM algorithm framework can be described as

$$\{\alpha^{k+1}, \mathbf{\Phi}^{k+1}\} = \underset{\alpha, \mathbf{\Phi}}{\text{argmin}} \ \mathcal{L}(\alpha, \mathbf{\Phi}, \{\mathbf{\Phi}_n^k, \mathbf{\Lambda}_n^k | n \in \mathcal{T}\}), \tag{14a}$$

$$\mathbf{\Phi}_n^{k+1} = \underset{\mathbf{\Phi}_n}{\text{argmin}} \ \mathcal{L}_n(\mathbf{\Phi}^{k+1}, \mathbf{\Phi}_n, \mathbf{\Lambda}_n^k), \ n \in \mathcal{T}, \tag{14b}$$

$$\mathbf{\Lambda}_n^{k+1} = \mathbf{\Lambda}_n^k + \rho_n (\mathbf{\Phi}_n^{k+1} - \mathbf{\Phi}^{k+1}), n \in \mathcal{T}. \tag{14c}$$

Since $h(\alpha, \mathbf{\Phi})$ and $f_n(\mathbf{\Phi}_n)$ are non-convex, (14a) and (14b) are difficult to be solved directly. But we can find that $\nabla h(\alpha, \mathbf{\Phi})$ and $\nabla f_n(\mathbf{\Phi})$ are Lipschitz continuous with the constant $L > \max\{2p, 4\omega^2 M^3 N |\hat{\Theta}|\}$ and $L_n > 4\omega_c^2 K^2 M^2 N$ respectively. It means that the upper bound quadratic functions of $\mathcal{L}(\alpha, \mathbf{\Phi}, \{\mathbf{\Phi}_n^k, \mathbf{\Lambda}_n^k | n \in \mathcal{T}\})$ and $\mathcal{L}_n(\mathbf{\Phi}^{k+1}, \mathbf{\Phi}_n, \mathbf{\Lambda}_n^k)$ can be given by (15) and (16) respectively.

$$\begin{aligned} &\mathcal{U}(\alpha, \mathbf{\Phi}, \{\mathbf{\Phi}_n^k, \mathbf{\Lambda}_n^k | n \in \mathcal{T}\}) = h(\alpha^k, \mathbf{\Phi}^k) \\ &+ \langle \nabla_{\mathbf{\Phi}} h(\alpha^k, \mathbf{\Phi}^k), \mathbf{\Phi} - \mathbf{\Phi}^k \rangle + \langle \nabla_\alpha h(\alpha^k, \mathbf{\Phi}^k), \alpha - \alpha^k \rangle \\ &+ \frac{L}{2} (\|\mathbf{\Phi} - \mathbf{\Phi}^k\|_F^2 + |\alpha - \alpha^k|^2) + \sum_{n \in \mathcal{T}} \mathcal{U}_n(\mathbf{\Phi}, \mathbf{\Phi}_n^k, \mathbf{\Lambda}_n^k). \end{aligned} \tag{15}$$

$$\mathcal{U}_n(\mathbf{\Phi}^{k+1}, \mathbf{\Phi}_n, \mathbf{\Lambda}_n^k) = f_n(\mathbf{\Phi}^{k+1}) + \langle \mathbf{\Lambda}_n^k, \mathbf{\Phi}_n - \mathbf{\Phi}^{k+1} \rangle + \langle \nabla f_n(\mathbf{\Phi}^{k+1}), \mathbf{\Phi}_n - \mathbf{\Phi}^{k+1} \rangle + \frac{\rho_n + L_n}{2} \|\mathbf{\Phi}_n - \mathbf{\Phi}^{k+1}\|_F^2. \tag{16}$$

Based on (14), (15) and (16), we propose a customized consensus-ADMM algorithm summarized in the following table.

Algorithm 1 The proposed consensus-ADMM algorithm

1: Initialization: Compute Lipschitz constants L and $\{L_n | n \in \mathcal{T}\}$. Set $\{\mathbf{\Lambda}_n^1 | n \in \mathcal{T}\}$ and $\{\mathbf{\Phi}^1 = \mathbf{\Phi}_n^1 | n \in \mathcal{T}\}$.
2: **repeat**
3: $\quad (\alpha^{k+1}, \mathbf{\Phi}^{k+1}) = \underset{\alpha, \mathbf{\Phi}}{\operatorname{argmin}}\ \mathcal{U}(\alpha, \mathbf{\Phi}, \{\mathbf{\Phi}_n^k, \mathbf{\Lambda}_n^k\})$.
4: $\quad \mathbf{\Phi}_n^{k+1} = \underset{\mathbf{\Phi}_n}{\operatorname{argmin}}\ \mathcal{U}_n(\mathbf{\Phi}^{k+1}, \mathbf{\Phi}_n, \mathbf{\Lambda}_n^k), n \in \mathcal{T}$.
5: $\quad \mathbf{\Lambda}_n^{k+1} = \mathbf{\Lambda}_n^k + \rho_n(\mathbf{\Phi}_n^{k+1} - \mathbf{\Phi}^{k+1}), n \in \mathcal{T}$.
6: **until** some preset condition is satisfied.

It should be noted that for all $n \in \mathcal{T}$, the variables in step 4 and step 5 are independent of each other, which means $|\mathcal{T}|$ pair updates can be executed in parallel. This is the main difference between the proposed consensus-ADMM algorithm and previous works including [6], [8] and [10].

4. ANALYSIS AND IMPROVEMENTS

4.1. Convergence

We have the following theorem to show that the proposed consensus-ADMM algorithm converges to some stationary point under some wild condition. Due to limited space, the details of the proof will be given in a future paper.

Theorem 1: For all $n \in \mathcal{T}$, if penalty parameters ρ_n and Lipschitz constants L_n satisfy $\rho_n > 5L_n$, the proposed ADMM algorithm is convergent, i.e.,

$$\lim_{k\to\infty} \alpha^k = \alpha^*, \lim_{k\to\infty} \mathbf{\Phi}^k = \mathbf{\Phi}^*,$$
$$\lim_{k\to\infty} \mathbf{\Phi}_n^k = \mathbf{\Phi}_n^*, \lim_{k\to\infty} \mathbf{\Lambda}_n^k = \mathbf{\Lambda}_n^*.$$

and $(\alpha^*, \mathbf{\Phi}^*, \{\mathbf{\Phi}_n^* | n \in \mathcal{T}\})$ is some stationary point of problem (12).

4.2. Computational Complexity

Since $\mathcal{U}(\alpha, \mathbf{\Phi}, \{\mathbf{\Phi}_n^k, \mathbf{\Lambda}_n^k | n \in \mathcal{T}\})$ and $\mathcal{U}_n(\mathbf{\Phi}^{k+1}, \mathbf{\Phi}_n, \mathbf{\Lambda}_n^k)$ are strongly quadratic functions, their minimizers can be obtained by solving linear equations $\nabla \mathcal{U}(\alpha, \mathbf{\Phi}, \{\mathbf{\Phi}_n^k, \mathbf{\Lambda}_n^k | n \in \mathcal{T}\}) = 0$ and $\nabla \mathcal{U}_n(\mathbf{\Phi}^{k+1}, \mathbf{\Phi}_n, \mathbf{\Lambda}_n^k) = 0$, i.e.,

$$\alpha^{k+1} = \alpha^k - \frac{\nabla_\alpha h(\alpha^k, \mathbf{\Phi}^k)}{L}, \tag{17a}$$

$$\mathbf{\Phi}^{k+1} = \frac{L\mathbf{\Phi}^k - \nabla_{\mathbf{\Phi}} h(\alpha^k, \mathbf{\Phi}^k) + \sum_{n\in\mathcal{T}} (\mathbf{\Lambda}_n^k + \rho_n \mathbf{\Phi}_n^k)}{L + \sum_{n\in\mathcal{T}} \rho_n}, \tag{17b}$$

$$\mathbf{\Phi}_n^{k+1} = \mathbf{\Phi}^{k+1} - \frac{\nabla f_n(\mathbf{\Phi}^{k+1}) + \mathbf{\Lambda}_n^k}{\rho_n + L_n}. \tag{17c}$$

Observing (17), we see that the main computational cost of each ADMM iteration is dominated by the calculation $\nabla h(\alpha, \mathbf{\Phi})$ and $\nabla f_n(\mathbf{\Phi})$. For $\nabla h(\alpha, \mathbf{\Phi})$, it takes $\mathcal{O}(M^2(N + M^2))$ complex multiplications. As for $\nabla f_n(\mathbf{\Phi})$, its computing complexity can be efficiently obtained by $\mathcal{O}(KMN)$ complex multiplications. So the total computation complexity of the each ADMM iteration is rough $\mathcal{O}(\max\{K|\mathcal{T}|N, M^3, NM\}M)$.

4.3. Improvements

Speed up convergence: To improve the Algorithm 1's convergence rate, we can exploit the following AGD method.

$$\hat{\mathbf{\Phi}}_n^{k+1} = \underset{\mathbf{\Phi}_n}{\operatorname{argmin}}\, \mathcal{U}_n\left(\mathbf{\Phi}^{k+1}, \mathbf{\Phi}_n, \mathbf{\Lambda}_n^k\right), \tag{18a}$$

$$\mathbf{\Phi}_n^{k+1} = \hat{\mathbf{\Phi}}_n^{k+1} + \gamma_k \left(\hat{\mathbf{\Phi}}_n^{k+1} - \hat{\mathbf{\Phi}}_n^k\right), \ n \in \mathcal{T}. \tag{18b}$$

where $\gamma_k = \frac{k-1}{k+r-1}$. In γ_k, $r \geq 3$ is some preset constant.

Reduce complexity: For different $n_1, n_2 \in \mathcal{T}$, $\{\mathbf{\Phi}_{n_1}, \mathbf{\Lambda}_{n_1}\}$ and $\{\mathbf{\Phi}_{n_2}, \mathbf{\Lambda}_{n_2}\}$ are updated in parallel. This structure can allow us to update a part of elements in $\mathcal{T}$, which leads to SGD method to reduce computational complexity of each ADMM iteration.

Embedding the above two strategies into the Algorithm 1, we propose an improved consensus-ADMM algorithm in the following table.

Algorithm 2 The improved consensus-ADMM algorithm

1: Initialization: Compute Lipschitz constants L and $\{L_n | n \in \mathcal{T}\}$. Set $\{\mathbf{\Lambda}_n^1 | n \in \mathcal{T}\}$ and $\{\mathbf{\Phi}^1 = \mathbf{\Phi}_n^1 | n \in \mathcal{T}\}$.
2: **repeat**
3: $\quad (\alpha^{k+1}, \mathbf{\Phi}^{k+1}) = \underset{\alpha, \mathbf{\Phi}}{\operatorname{argmin}}\ \mathcal{U}(\alpha, \mathbf{\Phi}, \{\mathbf{\Phi}_n^k, \mathbf{\Lambda}_n^k | n \in \mathcal{T}\})$.
4: $\quad$ Select a subset $\mathcal{T}_k \subset \mathcal{T}$ randomly.[1]
5: $\quad$ If $n \in \mathcal{T}_k$, implement the followings in parallel
6: $\quad\quad$ Compute $\mathbf{\Phi}_n^{k+1}$ via (18).
7: $\quad\quad \mathbf{\Lambda}_n^{k+1} = \mathbf{\Lambda}_n^k + \rho_n(\mathbf{\Phi}_n^{k+1} - \mathbf{\Phi}^{k+1})$.
8: $\quad$ endif.
9: **until** some preset condition is satisfied.

5. SIMULATION RESULTS

We present numerical examples to illustrate the performance of the proposed ADMM algorithms. The parameters are set as $M = 8, 16$, $N = 32, 64, 128$ and $n \in [-16, 16]$. The set of the angle Θ covers $(-90°, 90°)$ with spacing $1°$. Two directions of interest $\theta_1 = -40°$ and $\theta_2 = 30°$ are considered. Three other state-of-the-art algorithms L-BFGS method [6], CA approach [8] and D-ADMM [10] algorithm are carried out for comparisons. The weights (ω, ω_c) are $(1, 10)$. The desired beampattern is

$$\bar{P}_\theta = \begin{cases} 1, & \theta \in [\theta_i - 10°, \theta_i + 10°], \ i = 1, 2, \\ 0, & \text{otherwise}. \end{cases}$$

[1]Usually, criteria of selecting $\mathcal{T}_k$ is to guarantee every element in $\mathcal{T}$ is implemented equally in probability.

Table 1. Comparisons of MSE.

	(N, M)	$(128, 16)$	$(128, 8)$	$(64, 16)$	$(64, 8)$	$(32, 8)$
MSE	CA approach	1.9×10^{-2}	3.1×10^{-2}	1.9×10^{-2}	3.1×10^{-2}	3.1×10^{-2}
	L-BFGS	1.6×10^{-2}	3.0×10^{-2}	1.6×10^{-2}	3.0×10^{-2}	3.0×10^{-2}
	D-ADMM	/	2.9×10^{-2}	1.5×10^{-2}	3.0×10^{-2}	2.9×10^{-2}
	consensus-ADMM	1.5×10^{-2}	2.9×10^{-2}	1.5×10^{-2}	3.0×10^{-2}	3.0×10^{-2}

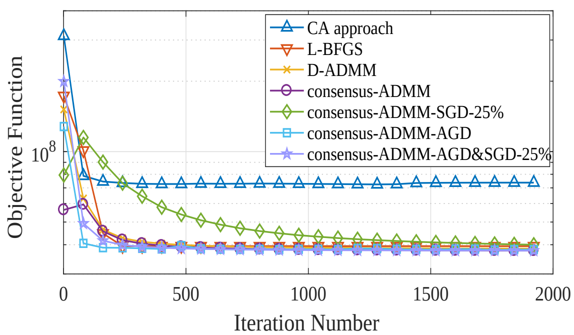

Fig. 1. Comparisons of the convergence performance.

We set the maximum iteration number to be 2000. The parameter r in AGD method is 3.

Figure 1 plots convergence curves of the algorithms in L-BFGS [6], CA approach [8], D-ADMM [10] and our proposed consensus-ADMM algorithms. Here SGD-25% means that we update one fourth elements in set $\mathcal{T}$. From the figure, we see that ADMM-AGD algorithm enjoys the fastest convergence rate. In comparison, ADMM-SGD-25%'s convergence is a little bit slower. However, we should note that it has lower computational complexity.

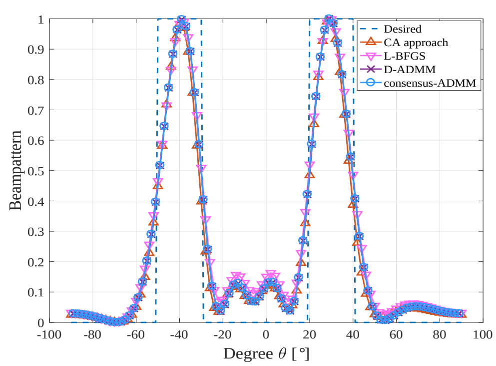

Fig. 2. Comparisons of the synthesized beampatterns with $N = 128$ and $M = 8$.

Table 1 lists the mean square error (MSE) between the designed beampattern and the desired one. From the table and Figure 2, we can see that the generated beampatterns of all four methods can approximate the desired beampattern very well. Here, we should note that the computation complexity of our proposed algorithm is $\mathcal{O}(\max\{K|\mathcal{T}|N, M^3, NM\}M)$, which is similar to L-BFGS method and D-ADMM, but much lower than CA approach. However, we should note that our proposed algorithm can be implemented in parallel. It means that it is much more suitable, especially for large-scale applications, than the other three algorithms from a practical point of view.

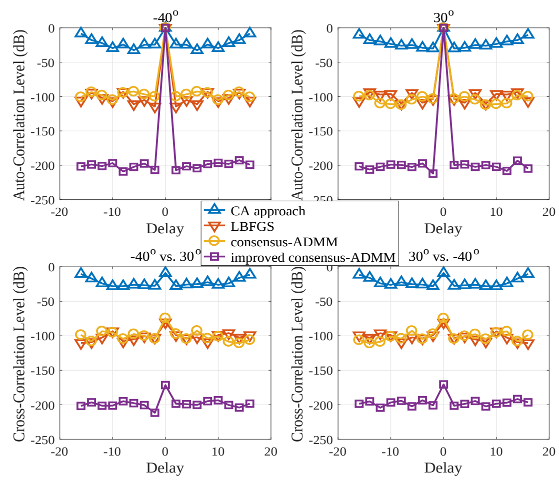

Fig. 3. Comparisons of the normalized spacial auto-/cross-correlation levels with $N = 128$ and $M = 8$.

Figure 3 shows the normalized auto-/cross-correlation levels of the different algorithms for interval $[-16, 16]$. From the figure, we can see that the proposed consensus-ADMM algorithms enjoy the best correlation levels performance among all algorithms.

6. CONCLUSION

In this paper, we design constant modulus probing waveforms with low correlation sidelobes for colocated MIMO radar. Through exploiting the structure of the problem, we exploit ADMM techniques to solve the corresponding nonconvex consensus problem approximately. We show that the proposed ADMM algorithm is guaranteed convergent to its stationary point. Moreover, parallel implementation structure indicates that the proposed consensus-ADMM algorithms are suitable for large scale applications. Numerical examples demonstrate their effectiveness.

7. REFERENCES

[1] J. Li and P. Stoica, *MIMO Radar Signal Processing.* Hoboken, NJ, USA: Wiley, 2009.

[2] J. Li and P. Stoica, "MIMO radar with colocated antennas," *IEEE Signal Process. Mag.*, vol. 24, no. 5, pp. 106-114, Sep. 2007.

[3] A. M. Haimovich, R. S. Blum, and L. J. Cimini, "MIMO radar with widely separated antennas," *IEEE Signal Process. Mag.*, vol. 25, pp. 116-129, Jan. 2008.

[4] P. Stoica, J. Li, and X. Zhu, "MIMO radar with colocated antenna: Review of some recent work," *IEEE Signal Process. Mag.*, vol. 24, pp. 106-114, Sep. 2007

[5] P. Stoica, J. Li, and Y. Xie, "On probing signal design for MIMO radar," *IEEE Trans. Signal Process.*, vol. 55, no. 8, pp. 4151-4160, Aug. 2007.

[6] Y.-C. Wang, X. Wang, H. Liu, and Z.-Q. Luo, "On the design of constant modulus probing signals for MIMO radar," *IEEE Trans. Signal Process.*, vol. 60, no. 8, pp. 4432-4438, Aug. 2012.

[7] G. Hua, and S. S. Abeysekera, "MIMO radar transmit beampattern design with ripple and transition band control," *IEEE Trans. Signal Process.*, vol. 61, no. 11, pp. 2963-2974. Jun. 2013.

[8] J. Li, P. Stoica, and X.-Y. Zheng, "Signal synthesis and receiver design for MIMO radar imaging," *IEEE Trans. Signal Process.*, vol. 56, no. 8, pp. 3959-3968, Aug. 2008.

[9] M. A. Kerahroodi, A. Aubry, A. De Maio, M. M. Naghsh and M. Modarres-Hashemi, "A coordinate-descent framework to design low PSL/ISL sequences," *IEEE Trans. Signal Process.*, vol. 65, no. 22, pp. 5942-5956, Nov. 2017.

[10] Z. Cheng, Z. He, S. Zhang and J. Li, "Constant Modulus Waveform Design for MIMO Radar Transmit Beampattern," *IEEE Trans. Signal Process.*, vol. 65, no. 18, pp. 4912-4923. Sep. 2017

[11] W. Su, S. Boyd, and E. J. Candes, "A differential equation for modeling nesterovs accelerated gradient method: Theory and insights," *Advances in Neural Information Processing Systems*, vol. 3, pp. 2510-2518, 2014.

[12] M. Hong, Z. Luo, and M. Razaviyayn, "Convergence analysis of alternating direction method of multipliers for a family of nonconvex problems," *SIAM Journal on Optimization*, vol.26, no. 1, pp. 337-364, 2016.